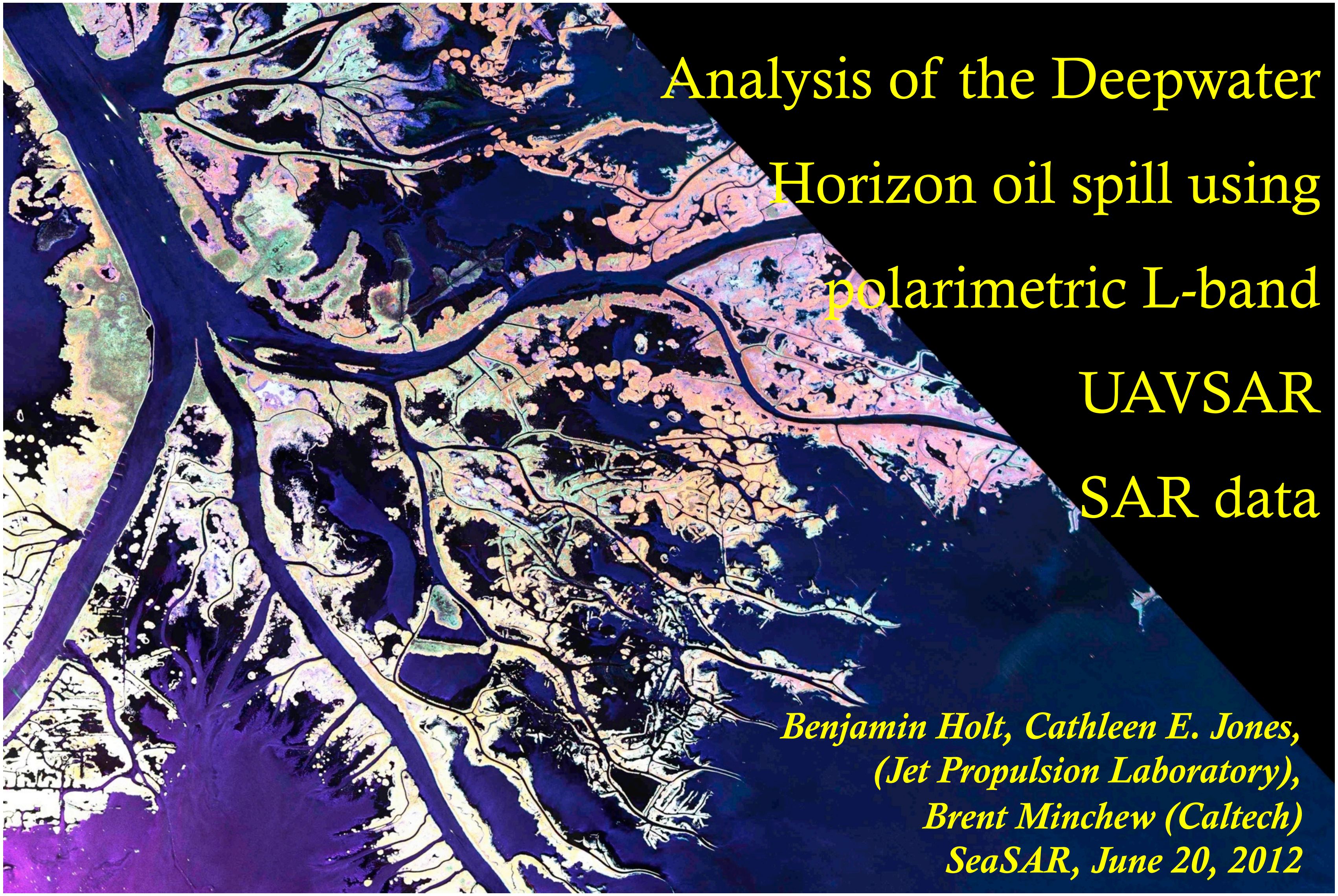

Analysis of the Deepwater Horizon oil spill using polarimetric L-band UAVSAR SAR data

Benjamin Holt, Cathleen E. Jones,
(Jet Propulsion Laboratory),
Brent Minchew (Caltech)
SeaSAR, June 20, 2012

References

All material shown is derived from these papers:

1. Minchew, Brent, Cathleen E. Jones Benjamin Holt (2012), **Polarimetric analysis of backscatter from the Deepwater Horizon oil spill using L-band radar**, DOI: 10.1109/TGRS.2012.2185804, to be published in TGRS.

2. Jones, Cathleen E., Brent Minchew, Benjamin Holt, and Scott Hensley (2011), **Studies of the Deepwater Horizon oil spill with the UAVSAR radar**, in *Monitoring and Modeling of the Deepwater Horizon Oil Spill: A Record-Breaking Enterprise*, Geophys. Monogr. Ser., vol. 195, edited by Y. Liu et al., pp. 33–50, AGU, Washington, D. C.

3. Leifer, I., B. Lehr, D. Simecek-Beatty, E. Bradley, R. Clark, P. Dennison, Y. Hu, S. Matheson, C. Jones, B. Holt, M. Reif, D. Roberts, J. Svejkovsky, G. Swayze, J. Wozencraft**, State of the art satellite and airborne marine oil spill remote sensing: Application to the BP Deepwater Horizon oil spill**, Remote Sensing of the Environment, 124, 185-209, 2012.

NOTE: All UAVSAR data available here http://www.asf.alaska.edu

Study Oil Spill Detection and the Impact of Oil Inundation in Wetland Ecosystems Using High Resolution Polarimetric L-band Radar

- Develop and validate algorithms for improved discrimination of oil slicks on water and collect data that will enable us to better determine oil properties from polarimetric radar backscatter returns.
- Study the use of radar for determining the extent of oil penetration into sensitive coastal ecological zones, in particular, to map the spread of oil from the coastline into coastal wetlands.
- Use the radar data to determine the extent and nature of the damage to different coastal ecosystems and to track ecosystem recovery.
- Combine optical and radar data for better detection and impact assessment (UAVSAR & AVIRIS).

NASA UAVSAR Gulf Oil Spill Campaign
22-23 June 2010 Deployment

- 2 days, 21 flight hours
- ~5500 km of flight lines with 22 km swath width
- imaged an area of 120,000 km^2

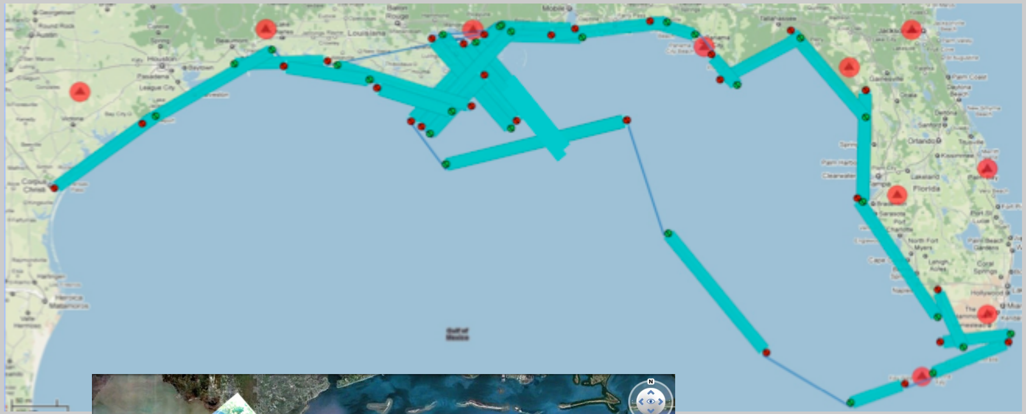

Frequency	L-Band 1217.5 to 1297.5 MHz (23.8 cm wavelength)
Intrinsic Resolution	1.7 m Slant Range, 0.8 m Azimuth
Polarization	HH, HV, VH, VV
Repeat Track Accuracy	± 5 meters
Transmit Power	> 3.1 kW
Radiometric Calibration	1.2 dB absolute, 0.5 dB relative channel-to-channel
Noise Floor	-47 dB average

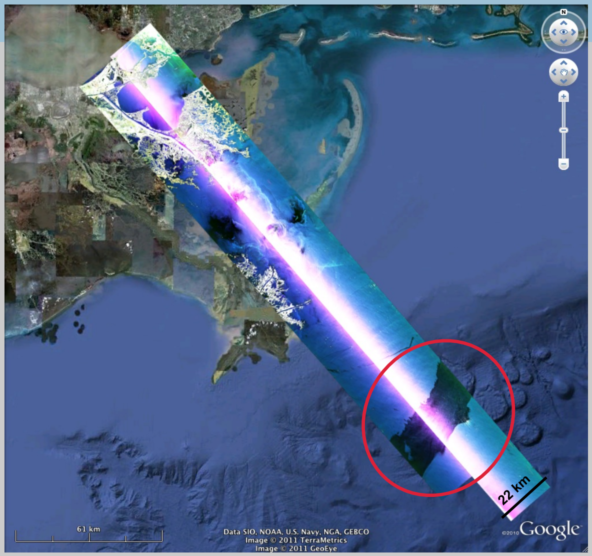

Main DWH oil slick, imaged 23 June 2010

B. Holt, C.Jones (JPL) , Minchew (Caltech)

Averaged Intensity Images

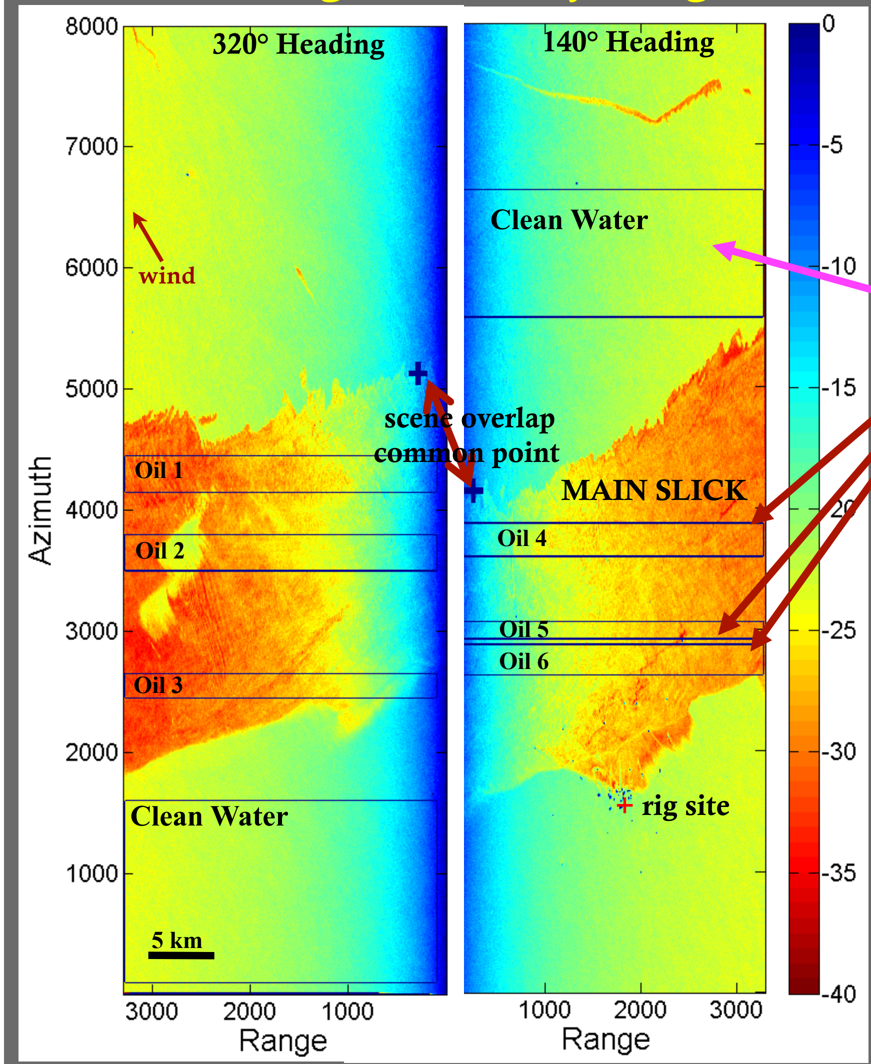

In the following slides, for each UAVSAR line the parameters are averaged in the along track direction and plotted as a function of incidence angle for a clean water region and for three strips within the slick.

Surface conditions:
sea state 1.0-1.3 m SWH
winds 2.5-5 m/s from 115°-126°

UAVSAR – L-Band Radar Study of the DWH Oil Spill
Variations in the Averaged Intensity within the main oil slick

NOT ONLY IS THE OIL SLICK CLEARLY DIFFERENTIATED FROM THE SURROUNDING WATER (DARK BLUE IN THE UAVSAR IMAGE), BUT THE LOW NOISE UAVSAR RADAR BACKSCATTER CAN DIFFERENTIATE SOME OIL CHARACTERISTICS WITHIN THE SLICK.

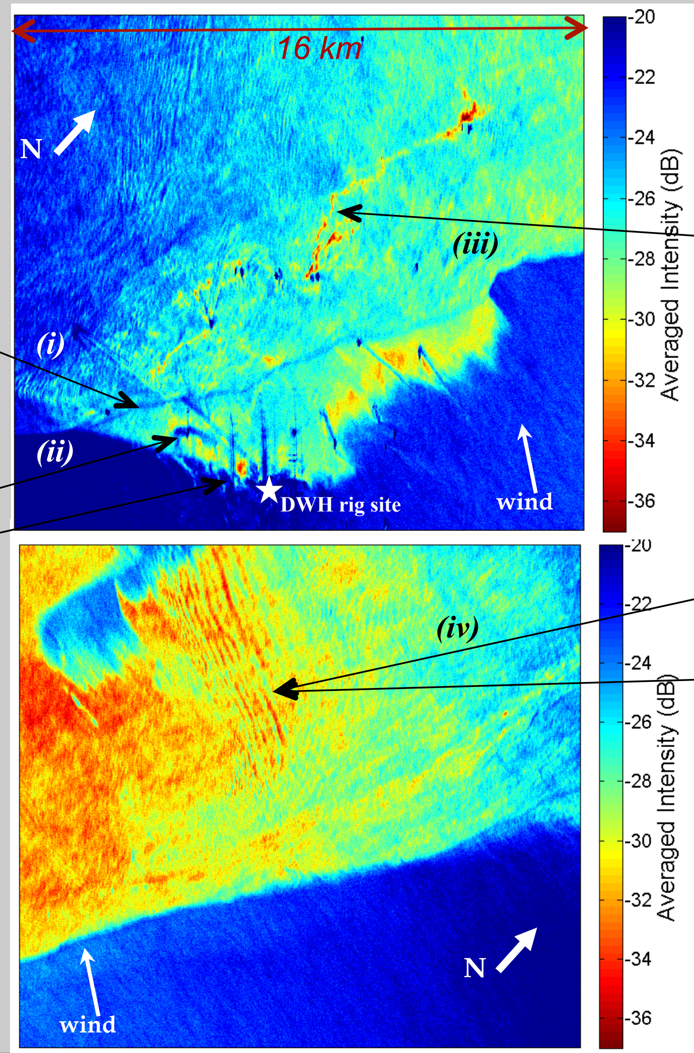

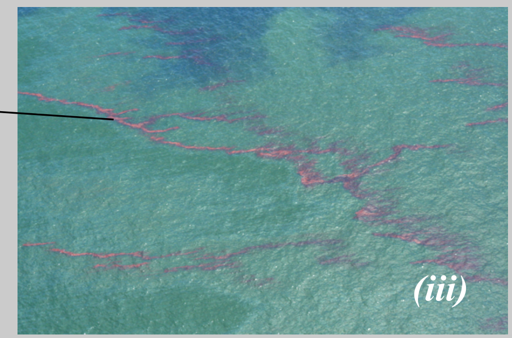

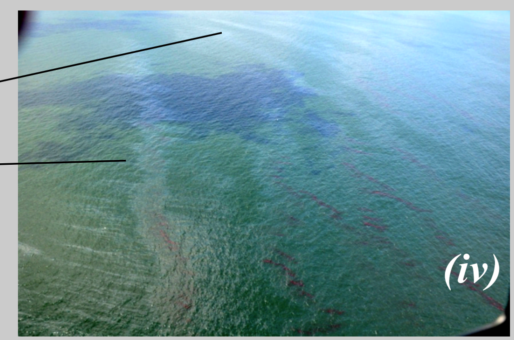

Photos taken over the slick on June 23, 2010, between 16:00 and 20:00 UTC (NOAA RAT-Helo and EPA/ASPECT), within hours of the UAVSAR overflight.

C. E. Jones, B. Holt, S. Hensley (JPL/Caltech) B. Minchew (Caltech), Studies of the Deepwater Horizon Oil Spill with the UAVSAR Radar, AGU Monograph Series, 2011

B. Holt, C.Jones (JPL) , Minchew (Caltech)

Radar Backscatter Polarization-Dependence

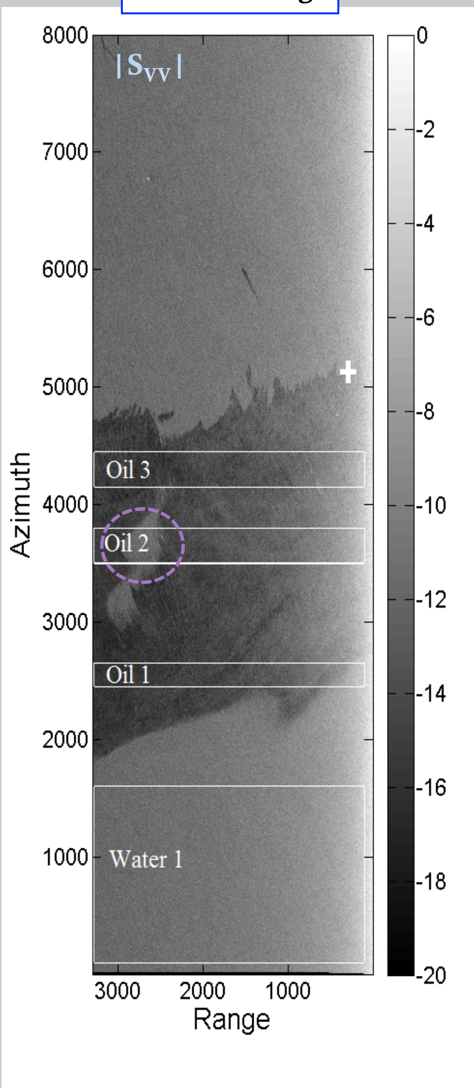

Polarimetric Returns vs. Incidence Angle

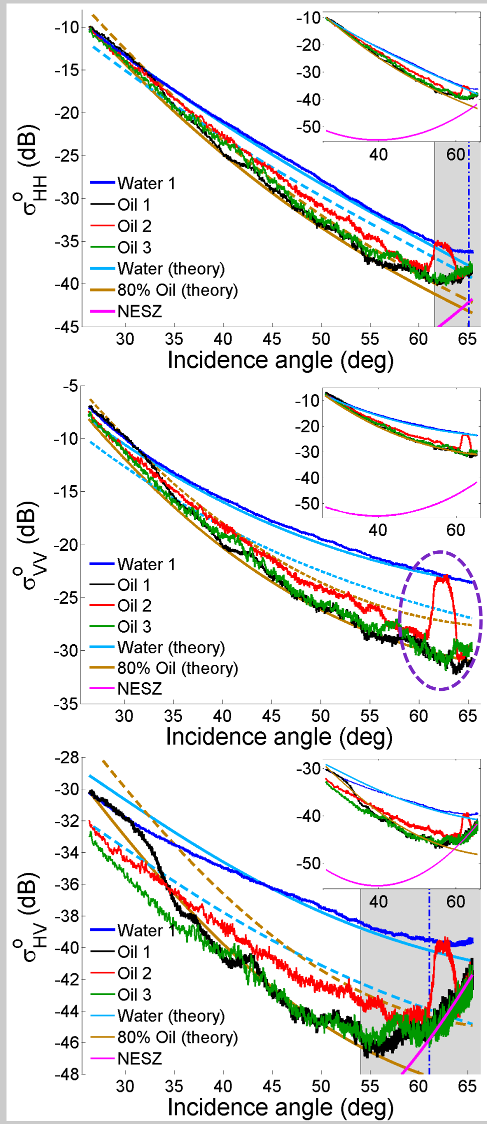

Bragg Scattering Theory

$$\sigma_{HH} = 4\pi k^4_{Bragg}\cos^4(\theta_i)\mathrm{W}(K_{ocean})\left|\left(\frac{\sin(\theta+\psi)\cos\beta}{\sin\theta_i}\right)^2 R_{HH} + \left(\frac{\sin\beta}{\sin\theta_i}\right)^2 R_{VV}\right|^2$$

$$\sigma_{VV} = 4\pi k^4_{Bragg}\cos^4(\theta_i)\mathrm{W}(K_{ocean})\left|\left(\frac{\sin(\theta+\psi)\cos\beta}{\sin\theta_i}\right)^2 R_{VV} + \left(\frac{\sin\beta}{\sin\theta_i}\right)^2 R_{HH}\right|^2$$

Damping of Ocean Waves by Oil

Alteration of Surface Dielectric Properties

For thick oil slicks we can derive the volumetric oil concentration from the change in dielectric of the scattering surface.

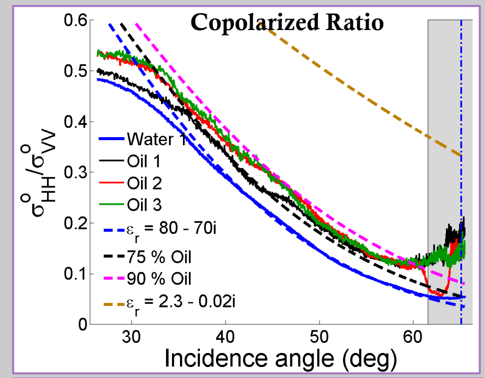

The ocean wave damping by the oil layer is measurable for all oil thicknesses.

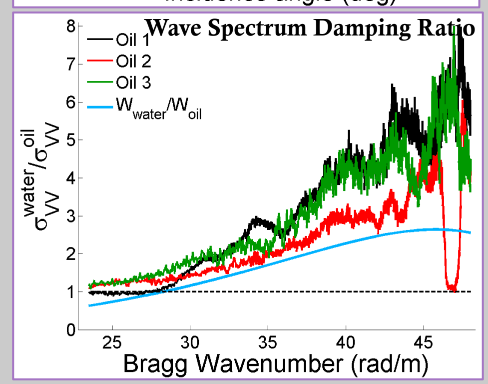

B. Minchew, C. E. Jones, B. Holt, Polarimetric analysis of backscatter from the Deepwater Horizon oil spill using L-band radar, TGRS, 2012, in print.

B. Holt, C.Jones (JPL) , Minchew (Caltech)

POLARIMETRIC DECOMPOSITION
ENTROPY, ANISOTROPY

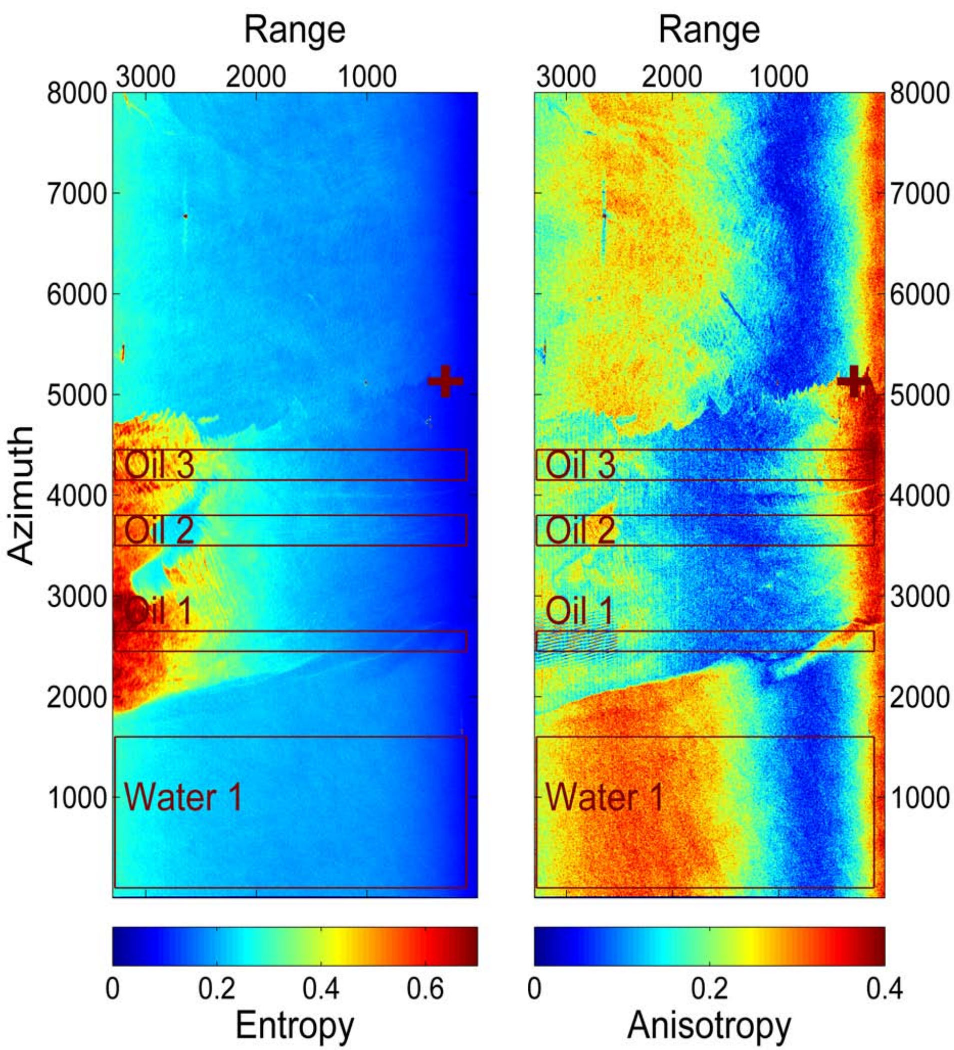

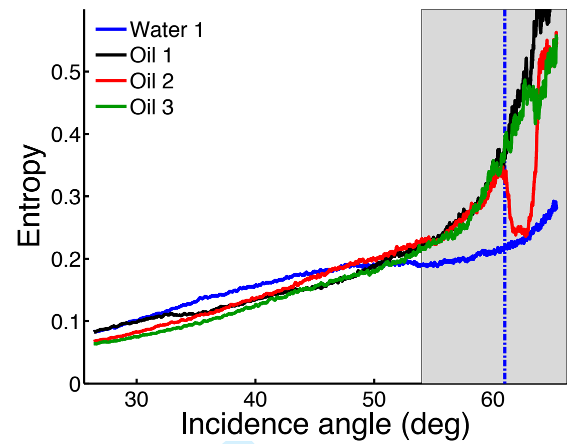

Dominant Scatterer <0.3

Entropy: Values are low (Bragg) except for low SNR regions (grey band - oil; blue line - H_2O)

Anisotropy: Shows greatest variation in the oil slick, but is only measurable with quad-pol, low noise instrument.

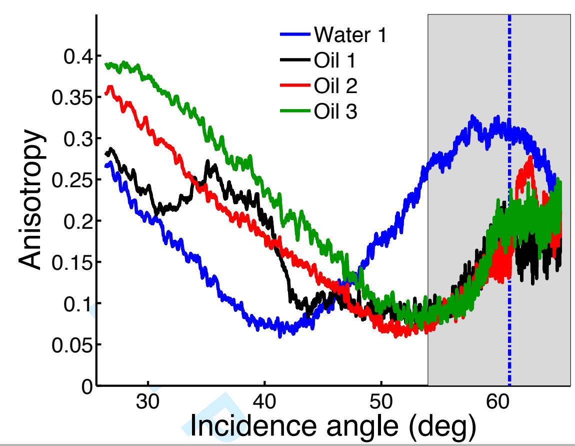

Roughness parameter

UAVSAR Validation Shoreline Impact Assessment, June 23-24, 2010

Bruce Davis *(DHS, Science and Technology Directorate),*
Philip Kuper, Kara Holekamp, Steve Tate *(Stennis Space Center)*

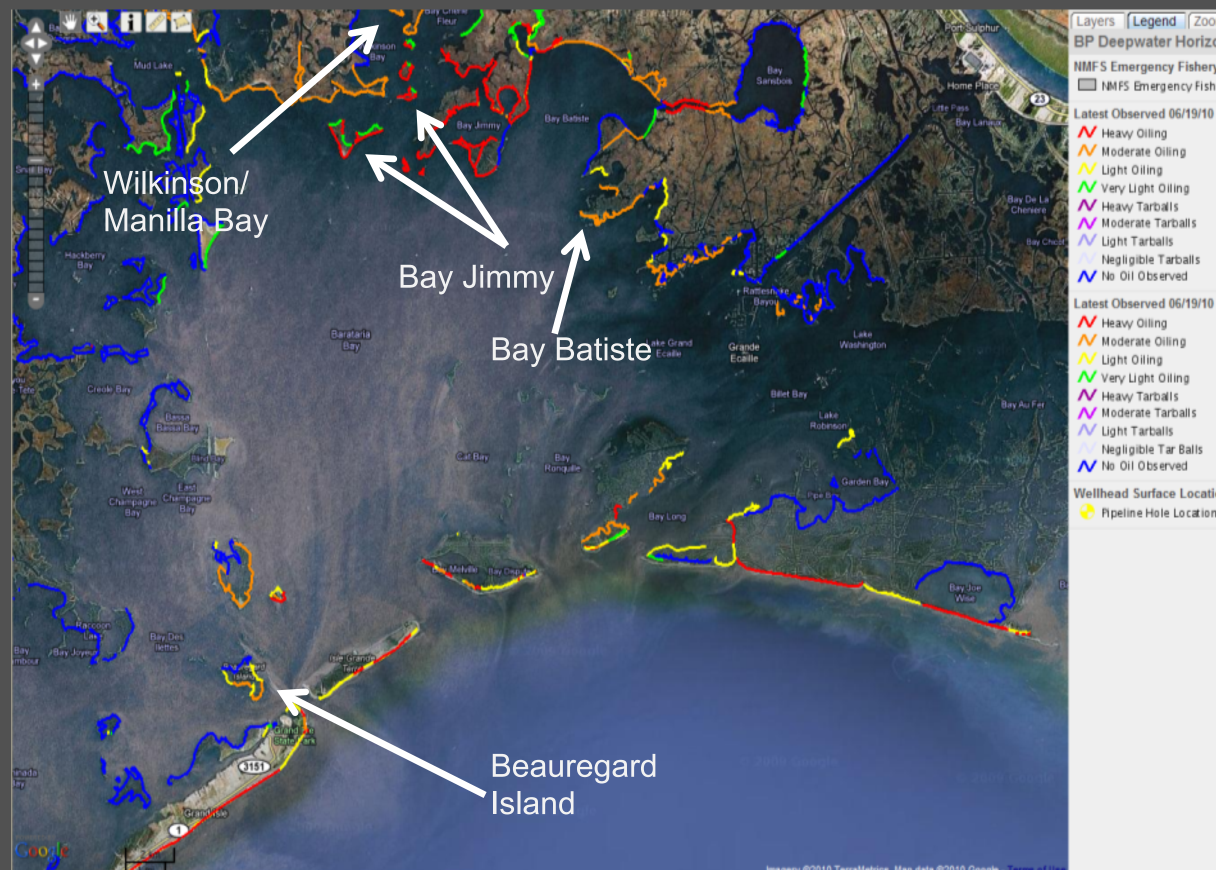

Shoreline Cleanup Assessment Team Map for June 23, 2010

UAVSAR – Oil Detection in Inland Waters
Comparisons of Fresh Oil at DWH Site and Weathered Oil in Barataria Bay

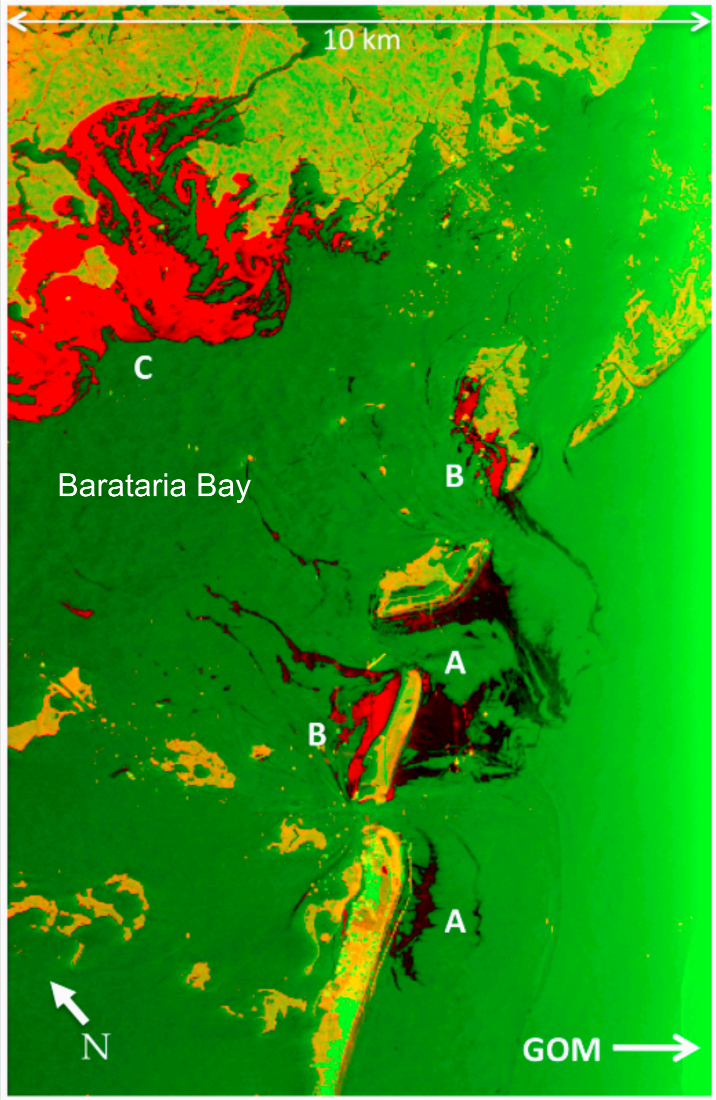

Large amounts of oil moved far into Barataria Bay in SE Louisiana on 16-17 June 2010, with oil remaining in the area until after the UAVSAR overflight.

Weathered oil in the interior of Barataria Bay shows a significantly lower intensity than oil around the rig site or in the Gulf of Mexico approaching the Louisiana shoreline. Observations made from boat in the bay indicate that the oil was present as sheen in the interior bay area at the time of the UAVSAR overflight.

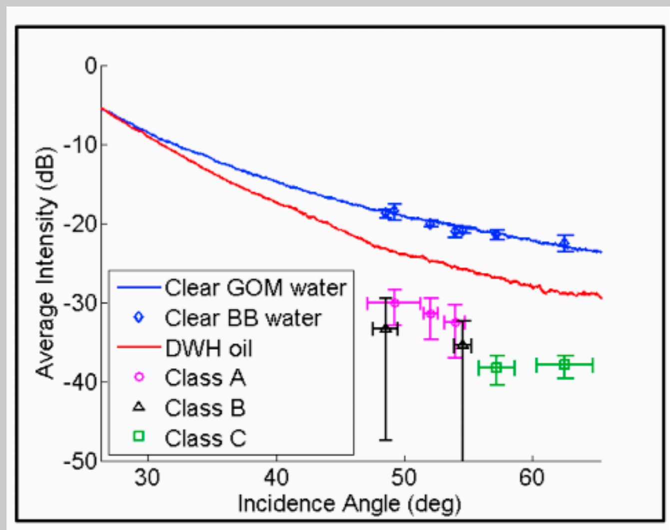

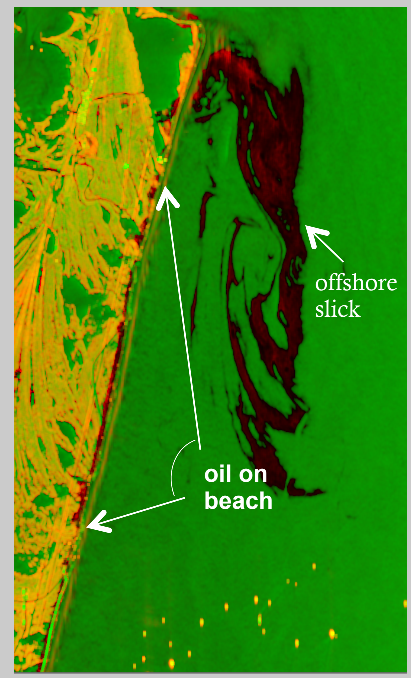

(1) C. E. Jones, B. Holt, S. Hensley (JPL/Caltech), B. Minchew (Caltech), Studies of the Deepwater Horizon Oil Spill with the UAVSAR Radar, AGU Monograph Series, 2011.
(2) E. Ramsey, A. Rangoonwala, Y. Suzuoki, & C. Jones, Oil Detection in a Coastal Marsh with POLSAR, Remote Sensing, 2012.

B. Holt, C.Jones (JPL) , Minchew (Caltech)

APPLICATION

MONITORING CONTAINMENT BOOMS FOR RAPID RESPONSE

C. E. Jones (Caltech/JPL), B. A. Davis (DHS) "High Resolution Radar for Response and Recovery: Monitoring Containment Booms in Barataria Bay," PE&RS, February 2011.

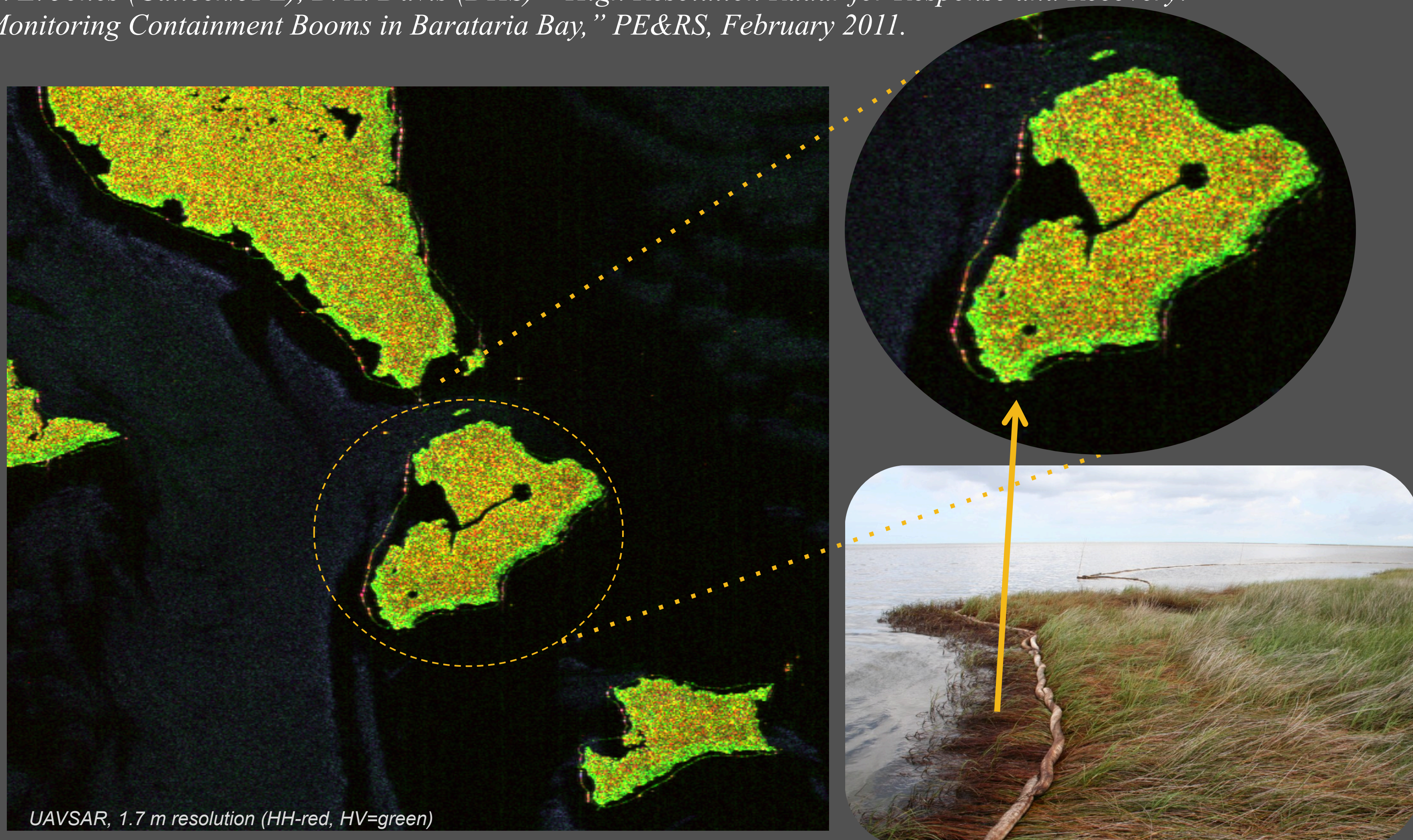

B. Holt, C.Jones (JPL) , Minchew (Caltech)

ERS-2 SAR, June 22, 2010, 0419 UTC

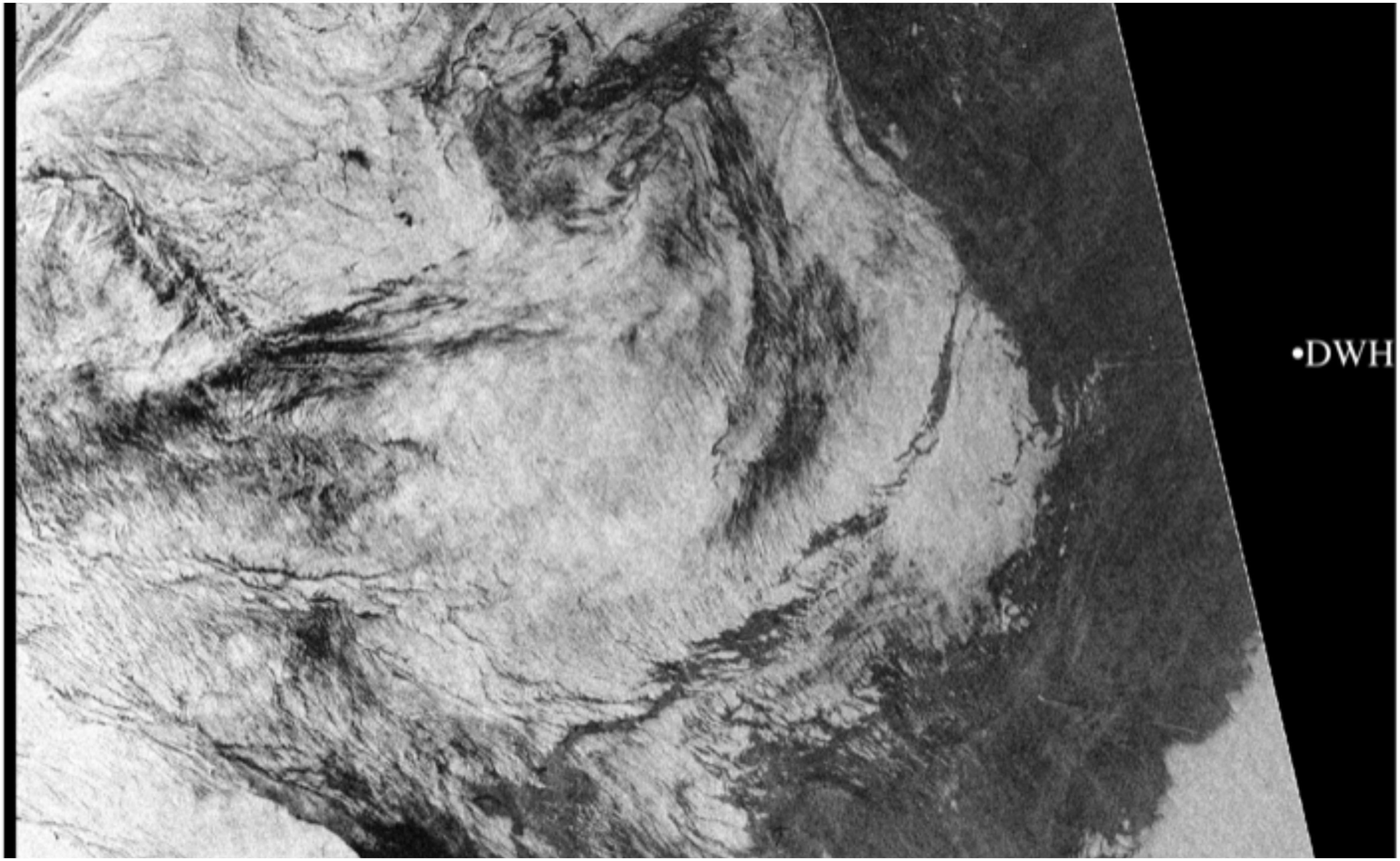

CSK1_VV_2010_0623_120845

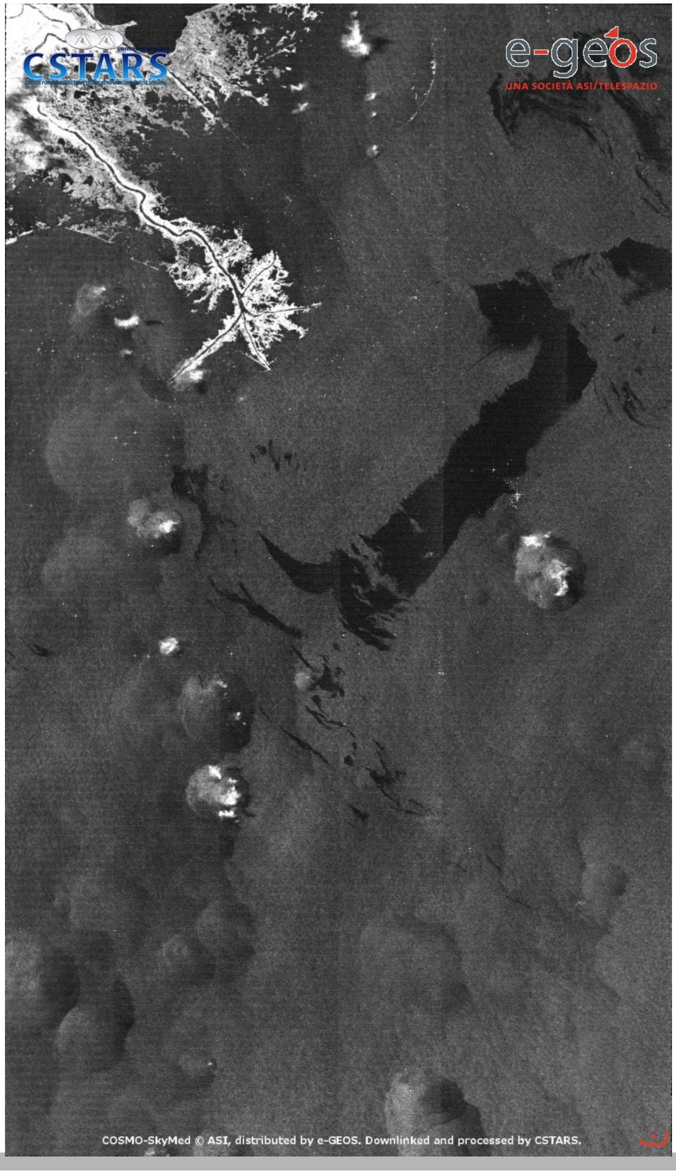

RS1_2010_0622_233708

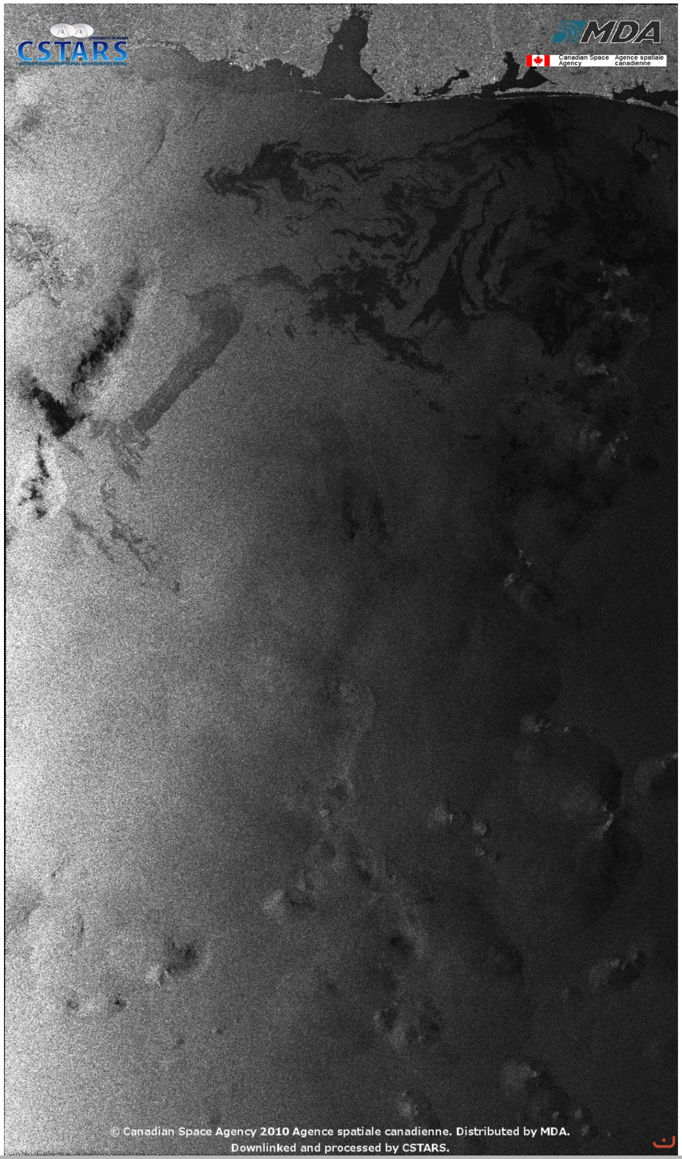

UAVSAR Instrument Noise Floor

UAVSAR NOISE FLOOR

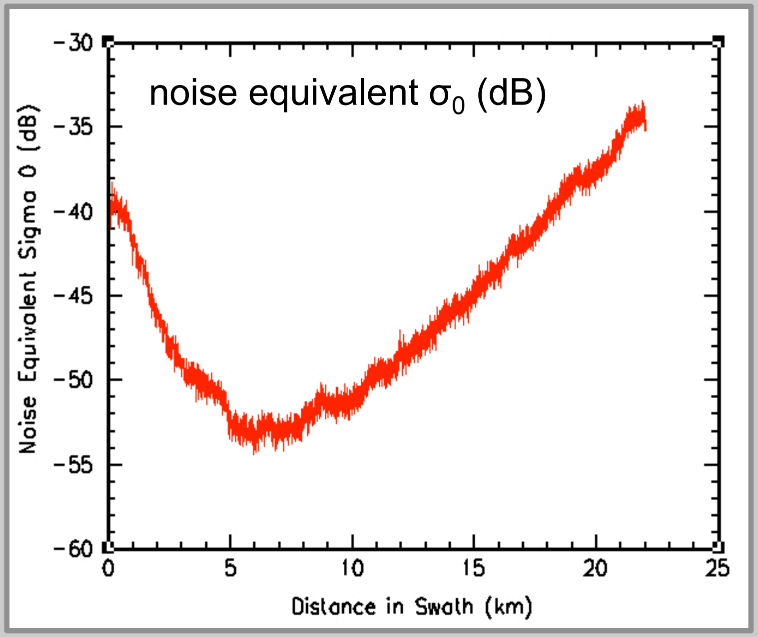

The low noise floor of the UAVSAR instrument makes it possible to measure the radar cross section from water with an L-band radar, even with oil damping the surface waves. We find that the instrument noise floor is reached only at the far edge of the swath for the HV returns from oil.

Comparison with other RADAR instruments

Sensor	Description (type, band, wavelength, polarization)	NESZ
UAVSAR	Airborne SAR; L-band (24 cm); quad polarization	-35 to -53 dB
ERS1/2	Satellite SAR; C-band; VV polarization	-20 to -29 dB[1]
Radarsat-2	Satellite SAR; C-band; single or dual polarization	-29 dB[2]
ENVISAT ASAR	Satellite SAR; C-band; single or dual polarization	-20 to -29 dB[1]
ALOS PALSAR	Satellite SAR; L-band; single, dual, or quad polarization	avg -23 dB (HH or VV), -26 dB (HV)[3]
TerraSAR-X	Satellite SAR; X-band;	avg -23 dB[4]
AIRSAR	Airborne SAR; C-, L-, and P-band; quad polarization	-34 to -50 dB (L); -40 to -48 dB (P); -26 to -34 dB (C)[5]

[1] http://envisat.esa.int/handbooks/asar/CNTR3-2-1.htm
[2] RadarSAT-2 Product Description, RN-SP-52-1238, 2-Nov-2009
[3] ALOS PALSAR Cyclic Report – Cycle 13, PALSAR_CR_13_070723_070907, 10-Jan-2008
[4] TerraSAR-X Ground Segment Basic Product Specification Document, TX-GS-DD-3302, 2008
[5] http://airsar.jpl.nasa.gov/documents/instrument.htm

C. Jones, B. Holt, S. Hensley (JPL/Caltech), B. Minchew (Caltech), Studies of the Deepwater Horizon Oil Spill with the UAVSAR Radar, AGU Monograph Series, 2011.

First Responders Primary Goals

•Detection of thickest oil, to guide containment and clean-up

•In US, primary observing tools are aircraft observers and associated imagery, followed by transport model.

•Satellite imagery used primarily for extent.

•NASA AVIRIS hyperspectral aircraft instrument detects thickness.

•Now it appears that NASA UAVSAR may detect thickness of emulsified

oil but what are limitations?

Deepwater Horizon MC 252, Gulf of Mexico

Type of Map: Overflight - Venice

Prepared by: NOAA (MG)

USE ONLY AS A GENERAL REFERENCE

Date/Time: 06-23-2010 / 0810-1005hrs CDT

Platform: Sikorsky S-76

Observers: Simecek-Beatty (NOAA) Del Valle (USCG)

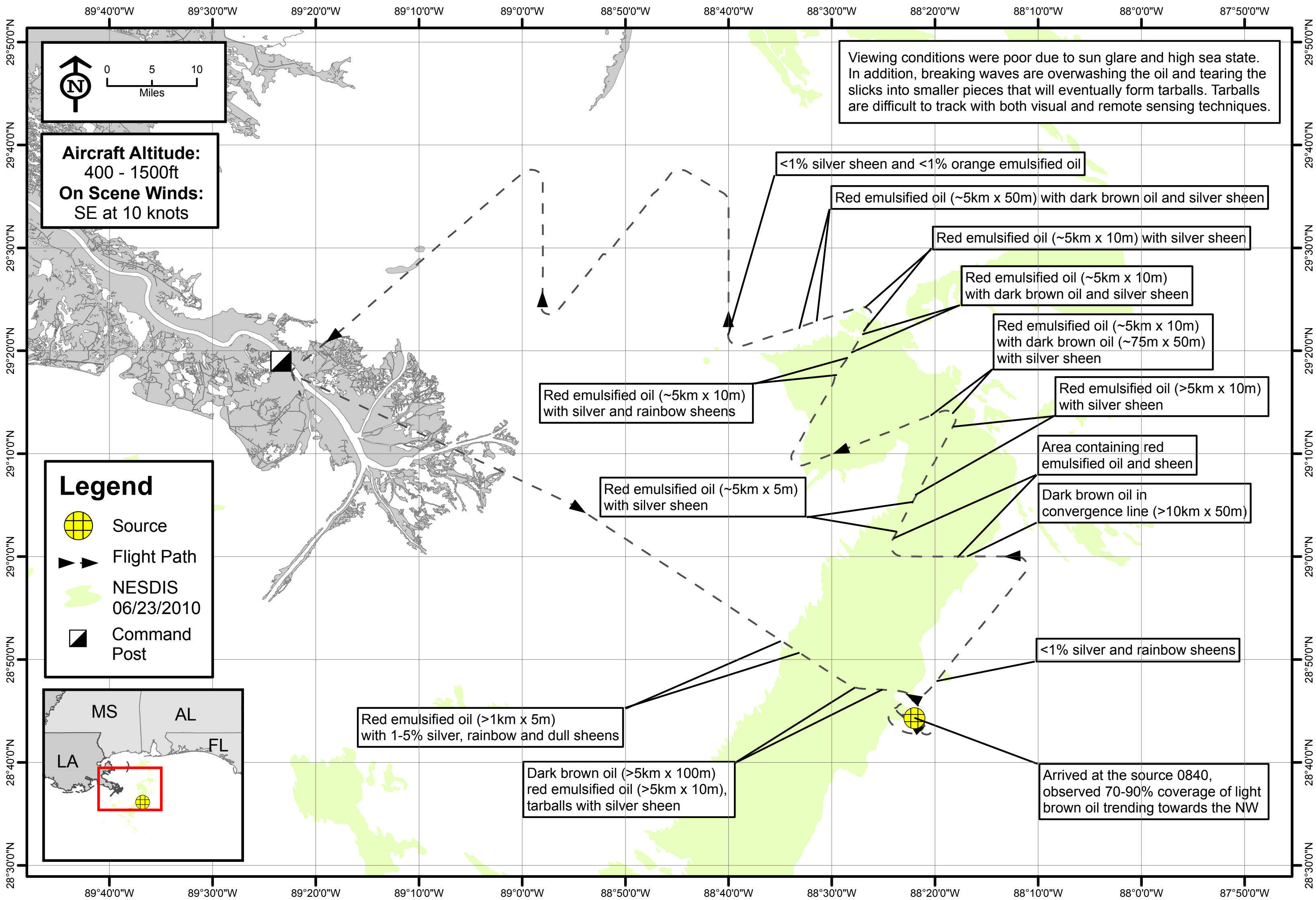

EXPERIMENTAL MARINE POLLUTION SURVEILLANCE DAILY COMPOSITE PRODUCT

Also available at: www.ssd.noaa.gov/PS/MPS/deepwater.html

VAILD ON: June 23, 2010 TIMES: 1205 - 0050 (6/24) UTC
ANALYST: EVANS
DATA SOURCES USED: COSMO SKYMED 1 & 2, RADARSAT 1, NASA MODIS TERRA

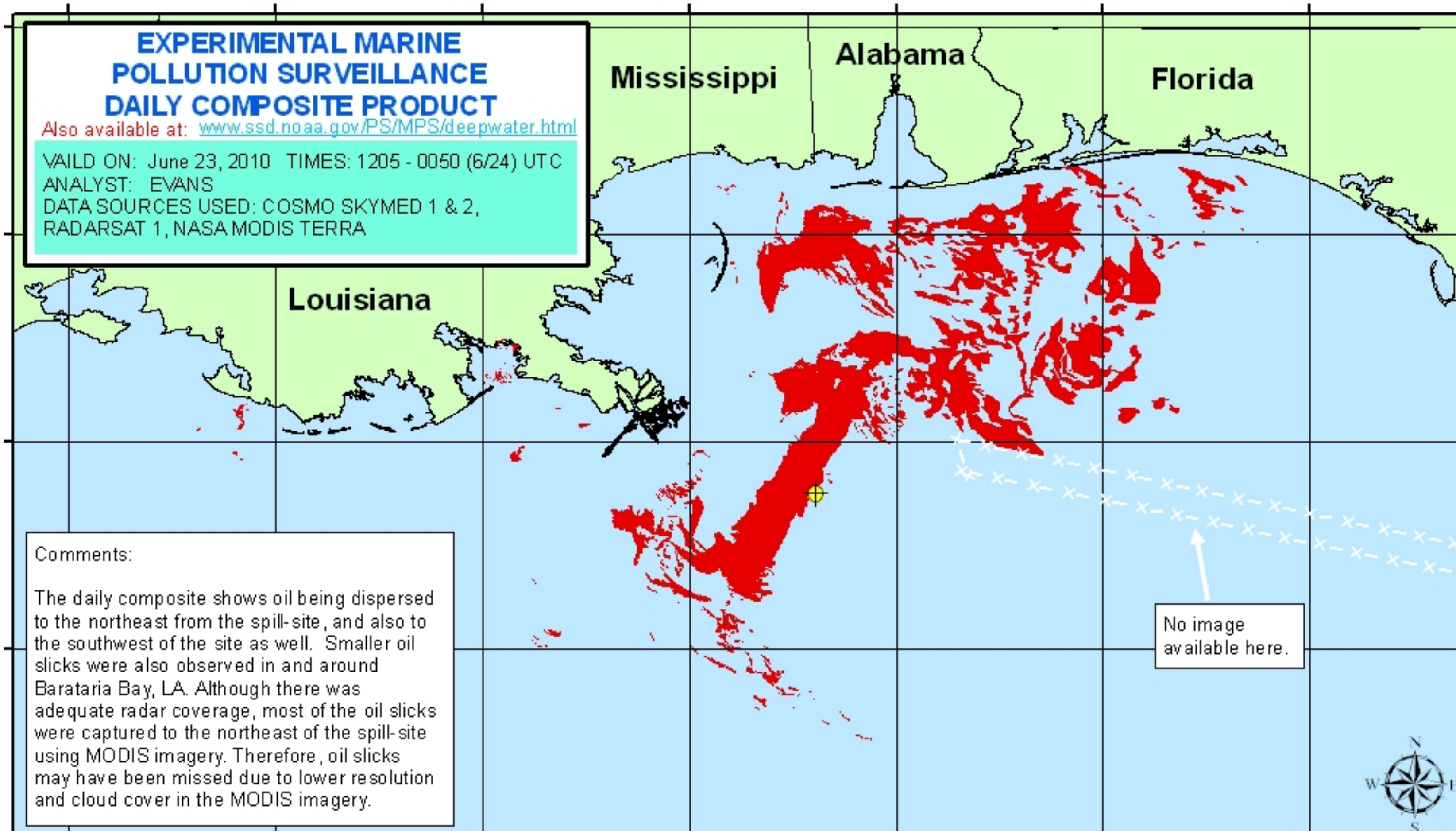

Comments:

The daily composite shows oil being dispersed to the northeast from the spill-site, and also to the southwest of the site as well. Smaller oil slicks were also observed in and around Barataria Bay, LA. Although there was adequate radar coverage, most of the oil slicks were captured to the northeast of the spill-site using MODIS imagery. Therefore, oil slicks may have been missed due to lower resolution and cloud cover in the MODIS imagery.

Analysis Provided by: The National Oceanic and Atmospheric Administration/National Environmental Satellite, Data and Information Service (NOAA/NESDIS)

This is an experimental product of the Satellite Analysis Branch and not operationally maintained. The outline of oil is a daily composite using a variety of satellite images and is based on an experimental pilot product and should be used with caution.

Legend

Possible Oil

Location of Deepwater Horizon Platform: [28°44'12" N / 88°23'14" W]

Miles: 0 12.5 25 50 75 100
Nautical Miles: 0 4 8 16 24 32
Kilometers: 0 15 30 60 90 120

CSTARS

© Canadian Space Agency/Agence spatiala canadienne (2010)
COSMO-SkyMed © ASI, distributed by e-GEOS. Processed by CSTARS.

AVIRIS Results

I. Leifer et al. / Remote Sensing of Environment 124 (2012) 185–209

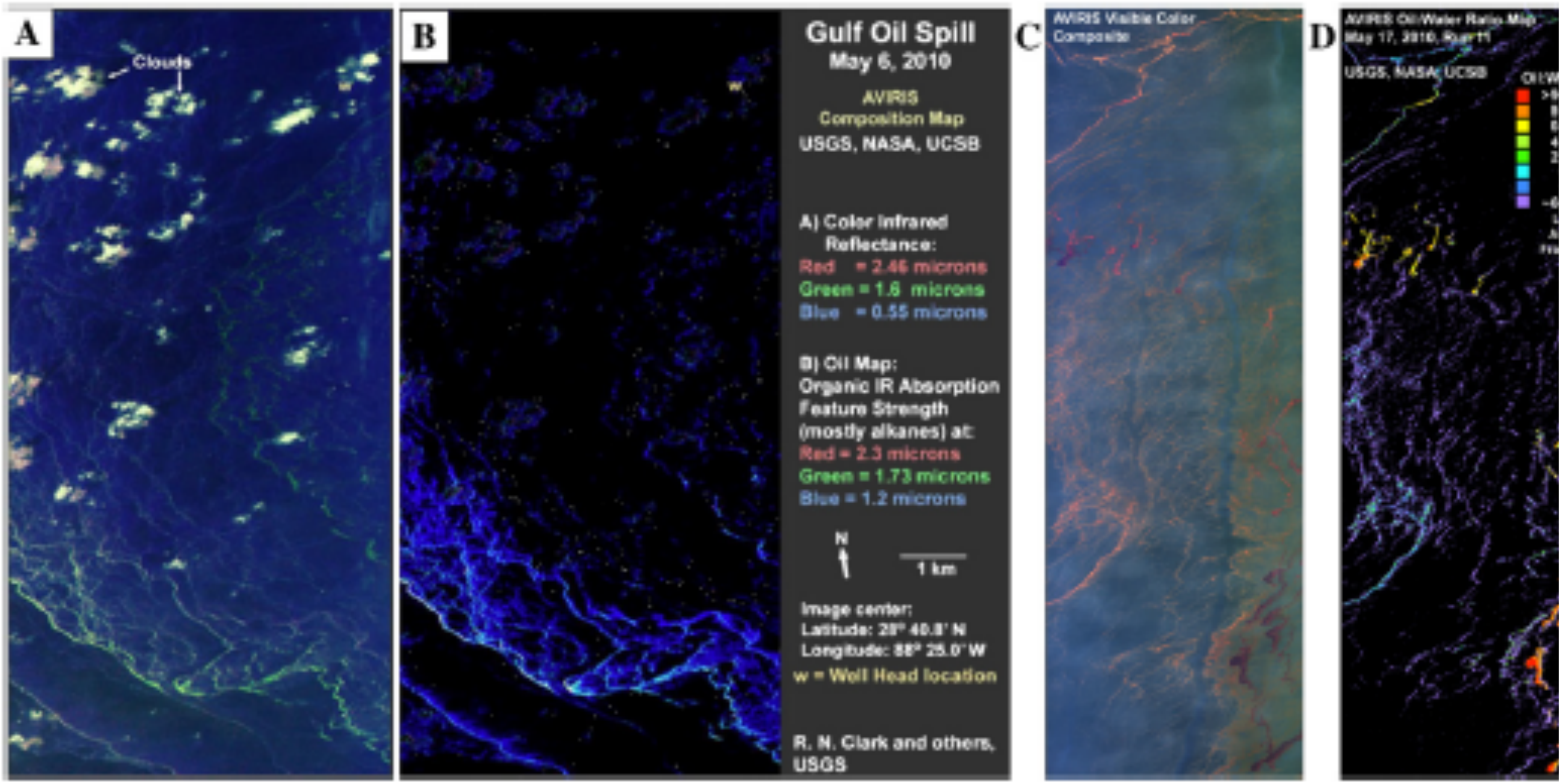

Fig. 9. A. False color AVIRIS image, including clouds in scene. B. RGB map of band absorption strength, which correlates with oil thickness. C. True color AVIRIS oil scene. D. T
corder oil-to-water emulsion ratio map.
From (Clark et al. 2010).

NOAA HAZMAT Guide

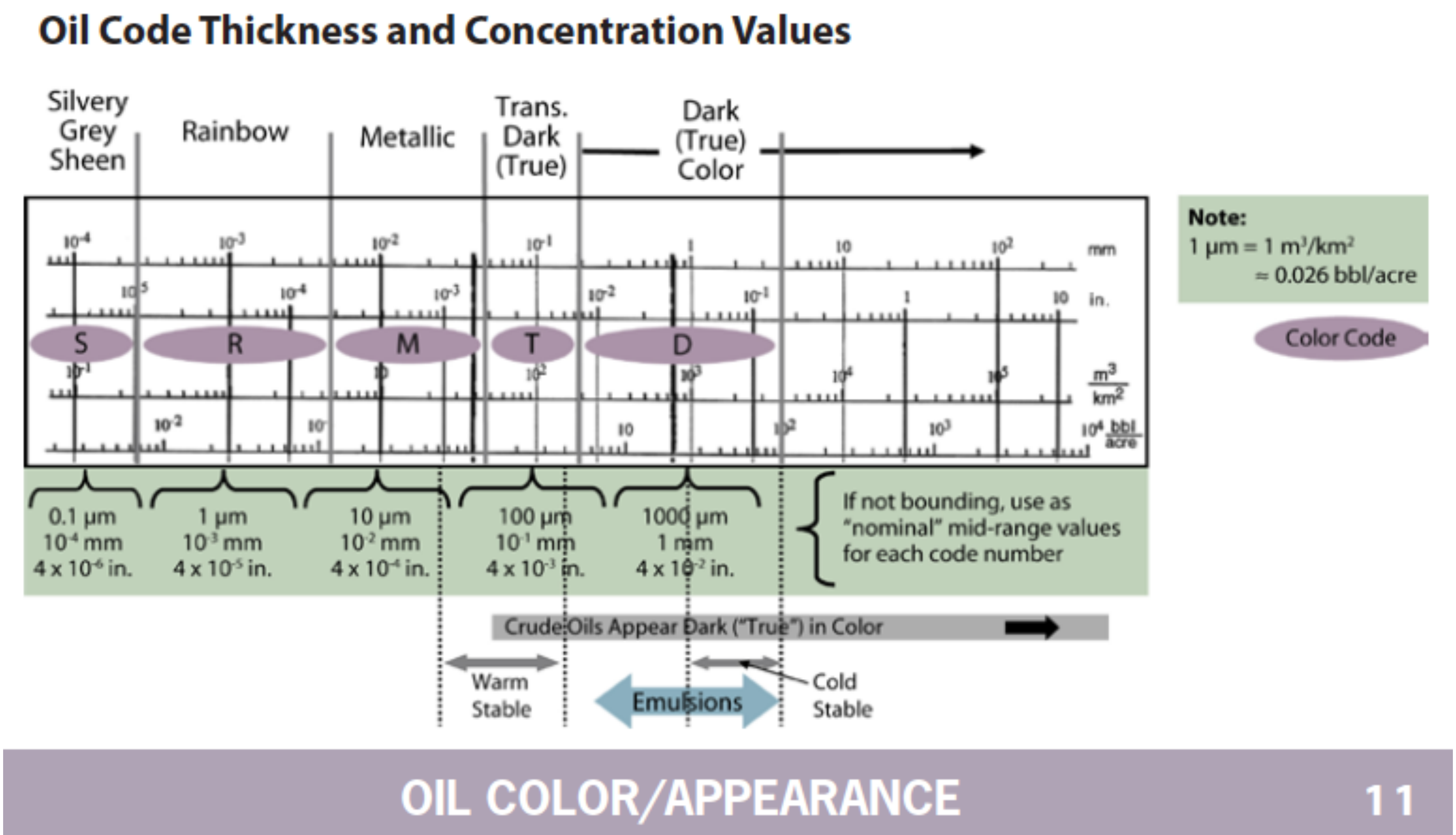

June 22, 2012 Near DWH

Photo taken by Oscar Garcia, Florida State Univ

Aerial Photography Locations – June 23, 2010

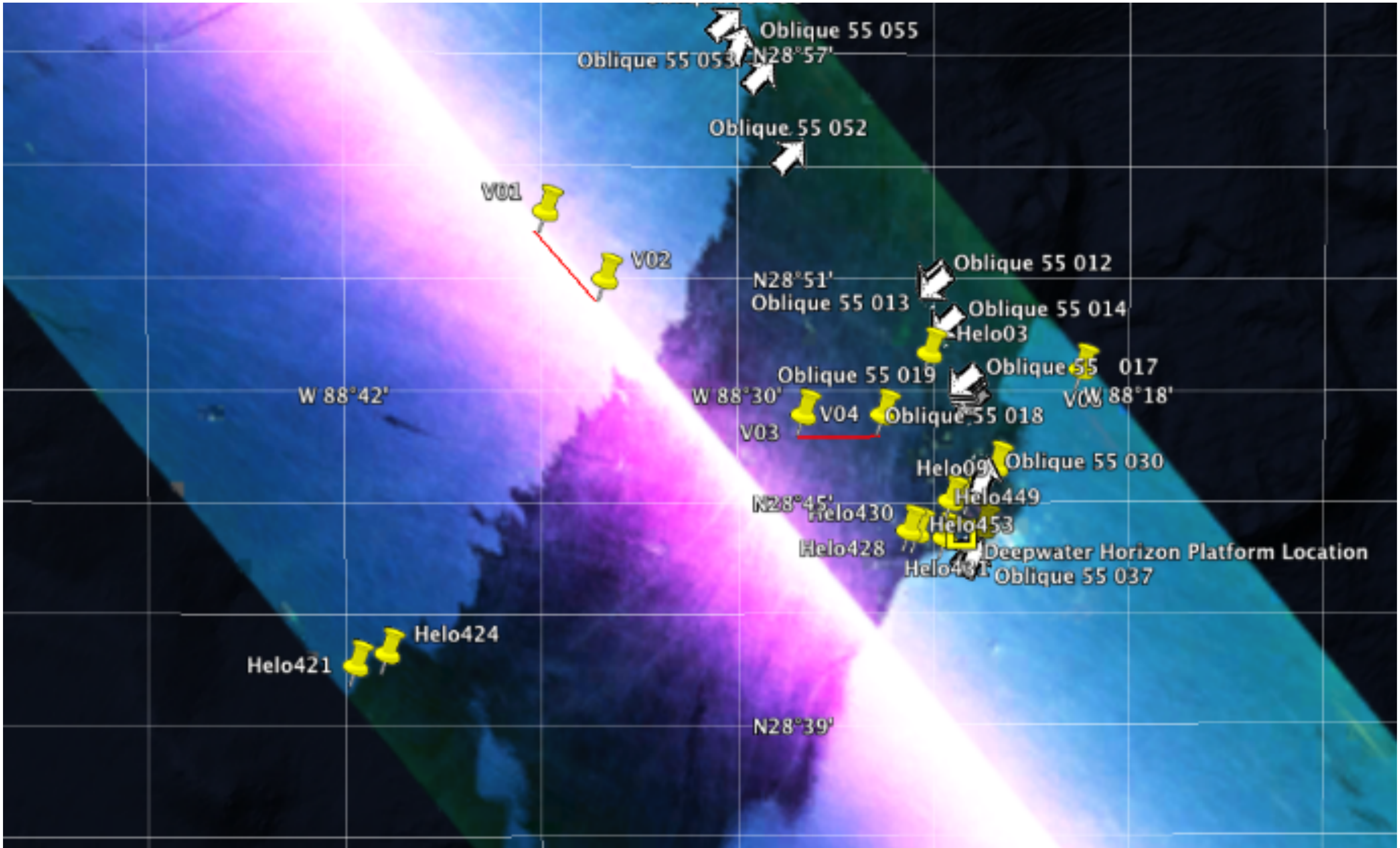

Aerial Photography

Conclusions

- UAVSAR provided unexpected valuable observations of oil spill properties related to thickness, from polarimetric analysis and due to low noise floor.

- Next step is to determine quantitative range of thickness that produces response, include additional data takes.

- Response based on tilted Bragg and dielectric mixture of oil-water. Is there non-Bragg response in oil present as well? Examine data related to wind and wave direction, i.e. leading and trailing edge.

(Ref: S. Ermakov, “On the intensification of decimeter-range wind waves in film slicks,” Izvestiya, Atmos. Ocean. Phys., vol. 46, no. 2, pp. 208–213, Apr. 2010.)

- Repeat UAVSAR flights of coastal wetlands to examine impacts of inundation on vegetation.

Back-up Slides

Effect of Surface Layer of Oil on Radar Backscatter from Water

Oil damps the small-scale capillary and gravity-capillary waves on the ocean surface mainly through a reduction in the surface tension at the gas-liquid interface.

Dispersion relationship for waves at the interface between air and a liquid of density ρ with surface tension σ:

$$\omega^2 = gk + (\sigma/\rho)k^3$$

gravity is the restoring force

surface tension and inertia are the restoring forces

$\rho_{oil}/\rho_{water} \approx 0.8 - 0.9$

$\sigma_{oil}/\sigma_{water} \approx 0.25 - 0.5$

$$v_{phase} = \sqrt{\frac{g}{k} + \frac{\sigma}{\rho}k}$$

for a given velocity, k increases when the surface tension decreases

Ocean waves are excited by resonant forcing in a turbulent wind field. The wavelength of capillary waves resonantly excited in the presence of oil is smaller than for a clean water-air interface, hence the damping of the smaller wavelengths. This affects the roughness scale of the water surface. In a real slick, the surface characteristics will vary between pure H20 and pure oil, depending upon layer thickness, oil type, and areal coverage.

Also, in viscoelastic fluids gravity waves with short wavelength are damped by restoring forces arising from gradients in the surface tension (Marongoni effect).

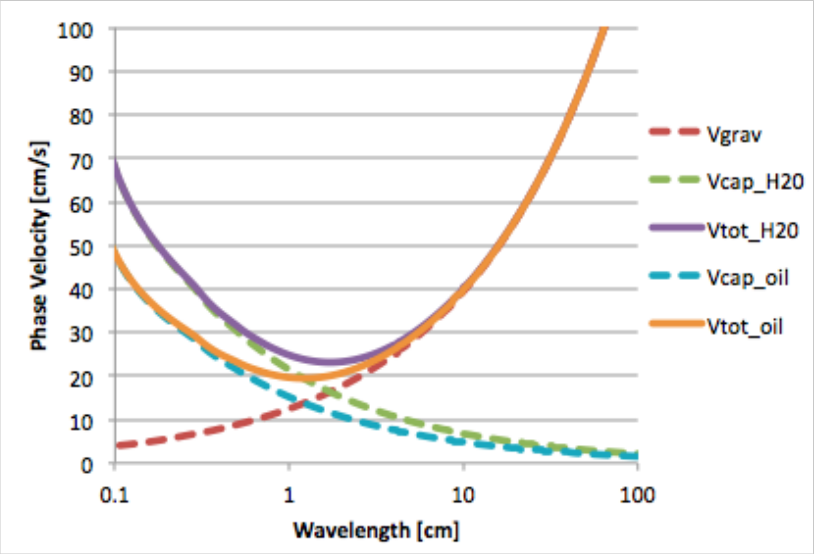

BRAGG SCATTERING THEORY

WAVE FACET MODEL

Radar backscatter from the ocean surface is dominated by scattering from small scale capillary and gravity-capillary waves that roughen the surface. In Bragg scattering theory, the dominant mechanism is resonant backscatter from surface waves of wave number k_{Bragg} where

$$k_{Bragg} = 2k\sin(\theta_{inc})$$

$$k = \frac{2\pi}{\lambda_{radar}}$$

As the incidence angle increases, the wavelength of the Bragg surface wave decreases to a minimum of λ_{radar}/2 at grazing angles.

L-band (λ_{radar}=23.8 cm) : λ_{Bragg} = 23.8 cm (30°), 13.7 cm (60°)

$$\sigma_{HH} = 4\pi k^4 \cos^4(\theta_i)\underbrace{\mathrm{W}(2k\sin(\theta+\psi), 2k\cos(\theta+\psi)\sin\beta)}_{\text{Ocean wave spectral density at Bragg wavelength}}\left|\left(\frac{\sin(\theta+\psi)\cos\beta}{\sin\theta_i}\right)^2 R_{HH} + \left(\frac{\sin\beta}{\sin\theta_i}\right)^2 R_{VV}\right|^2$$

$$\sigma_{VV} = 4\pi k^4 \cos^4(\theta_i)\mathrm{W}(2k\sin(\theta+\psi), 2k\cos(\theta+\psi)\sin\beta)\left|\left(\frac{\sin(\theta+\psi)\cos\beta}{\sin\theta_i}\right)^2 R_{VV} + \left(\frac{\sin\beta}{\sin\theta_i}\right)^2 R_{HH}\right|^2$$

$$\sigma_{HV} = 4\pi k^4 \cos^4(\theta_i)\mathrm{W}(2k\sin(\theta+\psi), 2k\cos(\theta+\psi)\sin\beta)\left|R_{VV} - R_{HH}\right|^2$$

$$\theta_i = \cos^{-1}[\cos(\theta+\psi)\cos(\beta)]$$

$$R_{VV} = \frac{(\varepsilon_r - 1)(\varepsilon_r(1+\sin^2(\theta_i)) - \sin^2(\theta_i))}{\left(\varepsilon_r\cos(\theta_i) + \sqrt{\varepsilon_r - \sin^2(\theta_i)}\right)^2} \qquad R_{HH} = \frac{\varepsilon_r - 1}{\left(\cos(\theta_i) + \sqrt{\varepsilon_r - \sin^2(\theta_i)}\right)^2}$$

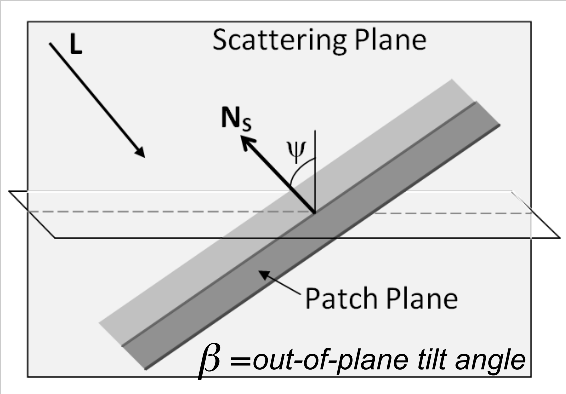

The Scattering Matrix relates the incident and scattered electric field vectors:

$$\begin{pmatrix} E_H \\ E_V \end{pmatrix}_{scattered} = \begin{pmatrix} S_{HH} & S_{HV} \\ S_{VH} & S_{VV} \end{pmatrix} \begin{pmatrix} E_H \\ E_V \end{pmatrix}_{incident}$$

The scattering matrix is expressed in the Pauli basis as

$$\begin{pmatrix} S_{HH} & S_{HV} \\ S_{VH} & S_{VV} \end{pmatrix} \xrightarrow{Pauli} k = \frac{1}{\sqrt{2}} \left[S_{HH} + S_{VV} \quad S_{HH} - S_{VV} \quad 2S_{HV} \right]^T$$

Diagonalization of the coherency matrix T=kk* gives 3 eigenvalues, λ, and eigenvectors, u. Those define the scattering mechanisms and their backscattered power.
The Cloude-Pottier polarimetric decomposition yields 4 variables derived from the eigenvalues and eigenvectors:

Entropy: $$H = \sum_{i=1}^{3} \left(\frac{\lambda_i}{\lambda_1 + \lambda_2 + \lambda_3} \right) Log_3 \left(\frac{\lambda_i}{\lambda_1 + \lambda_2 + \lambda_3} \right) \quad 0 \le H \le 1$$

Anisotropy: $$A = \frac{\lambda_2 - \lambda_3}{\lambda_2 + \lambda_3} \quad 0 \le A \le 1$$

Mean angle: $$\overline{\alpha}(u)$$

Averaged intensity: $$\Lambda = \sum_{i=1}^{3} \left(\frac{\lambda_i^2}{\lambda_1 + \lambda_2 + \lambda_3} \right)$$